Amino Acids (2024) 56:1
https://doi.org/10.1007/s00726-023-03379-x

ORIGINAL ARTICLE

Assessment of bioactive peptides derived from laminin-111 as prospective breast cancer-targeting agents

Fernanda Ferreira Mendonça[1] · Danielle Vieira Sobral[1] · Ana Claudia Ranucci Durante[1] · Ana Cláudia Camargo Miranda[2] · Jorge Mejia[2] · Daniele de Paula Faria[3] · Fabio Luiz Navarro Marques[3] · Marycel Figols de Barboza[2] · Leonardo Lima Fuscaldi[1] · Luciana Malavolta[1]

Received: 20 October 2023 / Accepted: 24 December 2023

Abstract

Breast cancer remains a pressing public health issue primarily affecting women. Recent research has spotlighted bioactive peptides derived from laminin-111, implicated in breast tumor development. Remarkably, the sequences IKVAV, YIGSR, and KAFDITYVRLKF from the α1, β1, and γ1 chains, respectively, have garnered significant attention. This study aims to assess the potential of these radiolabeled peptides as targeting agents for breast cancer. The three peptides were synthesized using the Fmoc strategy, purified via reversed-phase high-performance liquid chromatography (RP-HPLC), and characterized through mass spectrometry. Iodine-131 (^{131}I) radiolabeling was performed using the chloramine T method, exhibiting high radiochemical yield and stability for [^{131}I]I-YIKVAV and [^{131}I]I-YIGSR. Conversely, [^{131}I]I-KAFDITYVRLKF demonstrated low radiochemical yield and stability and was excluded from the biological studies. The lipophilicity of the compounds ranged from − 2.12 to − 1.10. Serum protein binding assay for [^{131}I]I-YIKVAV and [^{131}I]I-YIGSR reached ≅ 48% and ≅ 25%, respectively. Affinity for breast cancer cells was evaluated using MDA-MB-231 and MCF-7 tumor cell lines, indicating the affinity of the radiopeptides with these tumor cells. Ex vivo biodistribution profiles of the radiopeptides were assessed in the MDA-MB-231 breast tumor animal model, revealing tumor tissue accumulation, supported by a high tumor-to-contralateral muscle ratio and autoradiography. These results signify the effective penetration of YIKVAV and YIGSR into tumor tissue. Therefore, the synthesized α1 and β1 peptide fragments exhibit favorable characteristics as potential breast cancer-targeting agents, promising future exploration as radiopharmaceuticals for breast cancer.

Keywords Laminin 111-derived peptides · Targeting molecules · Radiolabeled peptides · Breast cancer

Introduction

Cancer stands as a significant and urgent global public health concern. In 2020, the Global Cancer Observatory reported a staggering 9.2 million newly diagnosed cancer cases and 4.4 million cancer-related death among females. For women, breast cancer emerges as the predominant malignancy, accounting for around 2.3 million fresh instances (24.5%) and 682 thousand fatalities (15.5%). This prominence of breast cancer underscores a substantial challenge within the public health system, given its high mortality rate (Batiston et al. 2011; Ferlay et al. 2021).

The progression of tumorigenesis and subsequent tumor development involves an intricate interplay of molecular changes (Montor et al. 2018). In the context of breast cancer, uncontrolled cellular growth gives rise to proliferative potential, sustained angiogenesis, and metastatic

Handling editor: F. Albericio.

✉ Luciana Malavolta
luciana.malavolta@gmail.com

[1] Department of Physiological Sciences, Santa Casa de Sao Paulo School of Medical Sciences, Rua Dr. Cesareo Motta Jr. 61, Sao Paulo CEP 01221-020, Brazil

[2] Hospital Israelita Albert Einstein, Sao Paulo 05521-200, Brazil

[3] Laboratory of Nuclear Medicine (LIM-43), Department of Radiology and Oncology, Faculdade de Medicina FMUSP, Universidade de Sao Paulo, Sao Paulo 01246-903, Brazil

Published online: 29 January 2024

competence (Hanahan and Weinberg 2011). Beyond the inherent modifications in tumor cells, the surrounding microenvironment significantly contributes to the carcinogenic process. A prime example is furnished by the laminin family of glycoproteins, which are a pivotal component of the extracellular matrix. While critical for tissue morphogenesis and homeostasis, laminins influence tumor invasion, angiogenesis, and metastasis (Ponce et al. 2001; Bosman and Stamenkovic 2003; Hamill et al. 2009).

Laminin-111, comprising α1, β1, and γ1 chains, is intricately linked to pivotal cellular processes, including adhesion, differentiation, proliferation, protease secretion, and metastasis within tumor cells. Additionally, bioactive peptides derived from laminin-111 have been identified as agents that influence the malignancy of tumors (Kikkawa et al. 2013; Otagiri et al. 2013).

Within the spectrum of biologically active peptides derived from laminin-111, a prominent role is assumed by the IKVAV peptide, sourced from the α1 chain. This peptide engenders cell adhesion and migration, thereby wielding a pivotal influence on tumor growth, metastasis, protease secretion, and angiogenesis across various tumor types (Sweeney et al. 1991; Bresalier et al. 1995; He et al. 2015). Extracted from the β1 chain, the CDPGYIGSR fragment emerges as a key entity associated with angiogenesis inhibition in diverse tumor contexts. Remarkably, subsequent investigations have illuminated that even the truncated YIGSR sequence retains its biological efficacy (Tashiro et al. 1989; Ponce et al. 2003; De Souza Santos 2011). Finally, the KAFDITYVRLKF sequence, known as the C16 peptide, represents the γ1 chain and is associated with an indelible imprint on gene expression in cells originating from invasive ductal carcinoma of the breast (MDA-MB-231) (Mokotooff et al. 1997; Smuczek et al. 2017).

As outlined in the literature, the laminin-111-derived peptides IKVAV, YIGSR, and KAFDITYVRLKF exhibit specific interactions with cell membrane receptors, namely integrins $\alpha_3\beta_1$ and $\alpha_6\beta_1$, 67 KD protein, and integrins $\alpha_v\beta_3$ and $\alpha_5\beta_1$, respectively (Kikkawa et al. 2013). Notably, the expression of these receptors is upregulated on the surface of tumor cells compared to their physiological presence on normal cell surfaces (Schottelius and Wester 2009). This divergence in expression levels suggests a potential avenue for employing these receptors as targets and the associated peptides as targeting agents for therapeutic or diagnostic interventions at tumor sites.

In this context, the present study aims at assessing the viability of peptides derived from the α1 (IKVAV), β1 (YIGSR), and γ1 (KAFDITYVRLKF) chains of laminin-111, radiolabeled with iodine-131 (^{131}I), as prospective targeting agents for breast cancer.

Materials and methods

Peptides synthesis

The YIKVAV (α1 chain), YIGSR (β1 chain), and KAFDITYVRLKF (γ1 chain) peptides were synthesized manually by Solid Phase Peptide Synthesis (SPPS) method, using the Fmoc strategy (Fields and Noble 1990), at 1.0 mmol scale on Wang resin (0.70 mmol/g). The amino acids and Wang resin were purchased from Bachem (Torrance, USA). The α-amino group deprotection was carried out using a solution containing 2 M 4-methyl-piperidine in dimethylformamide (DMF), with stirring for 20 min, at room temperature. The coupling reaction was carried out using 2.5 excess of Fmoc-amino acid in the presence of 2.5 mM N,N′-diisopropylcarbodiimide (DIC)/2.5 mM hydroxybenzotriazole (HOBt) in a 1:1 (v/v) dichloromethane (DCM)/DMF mixture as a solvent system. Each coupling reaction was qualitatively verified using the ninhydrin test (Kaiser et al. 1970) after 2 h. At the end of the synthesis, a cleavage reaction was performed in a highly concentrated trifluoracetic acid (TFA) solution.

Peptides characterization

All reagents and solvents meet the American Chemical Society standards or high-performance liquid chromatography (HPLC) grade.

Analytical and preparative RP-HPLC

The analyses and purification were conducted through RP-HPLC, using a C18 column (4.6 × 150 mm; particle size of 5 µm; pore size of 300 Å). Mobile phase A consisted of 0.1% TFA in H_2O, while mobile phase B was 0.1% TFA in 60:40 acetonitrile (ACN)/H_2O. The gradient profile for mobile phase B encompassed 5–95% in 30 min; flow rate of 1.0 mL/min for analytical purposes and 10.0 mL/min for purification purposes, with signal acquisition performed via a UV detector (λ = 220 nm).

Liquid chromatography mass spectrometry (LC–MS)

A system consisting of a micromass platform LCZ spectrometer, a Waters Alliance HPLC, a Waters 996 Photodiode Array detector and a Compaq workstation was used to characterize the synthesized peptides. A Waters Nova-Pak C18 column (2.1 × 150 mm; particle size of 3.5 µm; pore size of 60 Å) was employed, using the mobile phase A consisted of 0.1% TFA in H_2O, while mobile phase B was 0.1% TFA in 60:40 ACN/H_2O. The gradient profile for mobile

phase B encompassed 5–95% in 30 min; flow rate of 0.4 mL/min. The detection was at 220 nm over a mass range of 500–3930 Da.

Radiolabeling of peptides

The peptides were radiolabeled with ^{131}I through the utilization of [^{131}I]NaI and the chloramine T technique, as previously described (Durante et al. 2019). The ^{131}I was obtained as [^{131}I]NaI from Nordion (Ottawa, Canada) and distributed in Brazil by the *Instituto de Pesquisas Energéticas e Nucleares* of the *Comissão Nacional de Energia Nuclear—IPEN-CNEN* (Sao Paulo, Brazil). Briefly, the procedure involved introducing aliquots of approximately 11–15 MBq of [^{131}I]NaI, with pH 7 for YIKVAV and 9–10 for YIGSR and KAFDITYVRLKF, and 3–5 µL of 1 mg/mL (4.4 mM) chloramine T solution into a vial containing a 25 µg aliquot (~ 36 nmol, 42 nmol and 17 nmol, respectively) of each peptide dissolved in a 0.1 M phosphate buffer solution (PBS) at pH 7.4. After 1 to 4 min, at room temperature, 5 µL of a solution containing 2 mg/mL (0.01 M) sodium metabisulfite was added to interrupt the radioiodination reaction. Figure 1 shows the chemical structure of the peptides after the ^{131}I-labeling process.

The radiolabeling efficiency of the [^{131}I]I-peptides was evaluated through an ascending chromatography technique employing silica gel-coated plates on an aluminum base (TLC-SG). Various mobile phases were assessed to determine the peptide radiolabeling yield. Following standardization, the solvent system that yielded superior separation between the [^{131}I]I-peptides and [^{131}I]NaI was constituted of 95:5 ACN/H_2O for [^{131}I]I-YIKVAV and [^{131}I]I-YIGSR, whereas for [^{131}I]I-KAFDITYVRLKF the better mobile phase was 0.9% NaCl. After the chromatographic development, the distribution of radioactivity on the strip was determined using a radiation scanner. The retention factors (R_f) of [^{131}I]NaI and [^{131}I]I-peptides, along with the percentage of activity corresponding to the respective peaks, were ascertained.

The radiochemical yield was also assessed using RP-HPLC analyses. A C18 analytical column (3.0 × 100 mm; 2.6 µm) maintained at 30 °C by a column oven was employed. The mobile phase A consisted of 0.1% TFA in H_2O, while mobile phase B comprised 0.1% TFA in ACN. The gradient profile for mobile phase B encompassed the following proportions: 3–10% (0–2 min), 10–30% (2–16 min), and 30–5% (16–22 min); flow rate of 1.0 mL/min, with signal acquisition being performed via both a UV detector ($\lambda = 220$ nm) and a radioactivity detector. In the chromatographic analysis, the retention times (R_t) corresponding to unlabeled peptides, [^{131}I]NaI, and [^{131}I]I-peptides were determined.

Radiochemical stability

The radiochemical stability of the radiopeptides was evaluated in two distinct environments: in saline ($n = 3$), at room temperature and under refrigeration (4–8 °C), by a period of 48 h after the radiolabeling, and in serum ($n = 5$), at 37 °C, for up to 24 h after incubation. At predefined time intervals, aliquots were extracted and subjected to ascending chromatography, as previously detailed.

Lipophilicity

The lipophilicity was evaluated according to established methods (Durante et al. 2019). Briefly, 25 µL of each radiopeptide (0.6 MBq) were added into a blend of *n*-octanol (500 µL) and water (475 µL), and vortexing for 30 s, followed by centrifugation (5000 rpm) for 5 min ($n = 5$). From both phases, 100 µL aliquots were withdrawn and measured employing an automatic gamma counter. The lipophilicity was quantified as Log P value [Eq. (1)]:

$$P = log\left[\frac{cpm\,(\text{organic phase})}{cpm\,(\text{aqueous phase})}\right] \quad (1)$$

Serum protein binding (SPB)

The percentage of radiopeptides bound to serum proteins was quantified according to the literature (Sobral et al. 2020). Briefly, 25 µL of each radiopeptide (0.6 MBq) were added into 475 µL of serum and incubated (37 °C) under gentle agitation for 1 h ($n = 5$). Subsequently, 1 mL of 0.6 M trichloroacetic acid (TCA) was added, vortexing for 1 min, and the samples were centrifuged (4000 rpm) for 10 min. The supernatant and the pellet were separated, and the radioactivity in each fraction was measured in an automatic gamma counter. The SPB percentage was calculated as [Eq. (2)]:

$$SPB\,[\%] = \frac{cpm(pellet)}{cpm(pellet + supernatant)} \times 100 \quad (2)$$

Biological evaluation

Culture of breast cancer cells (MDA-MB-231 and MCF-7)

The human breast cancer cell lines were purchased from the *Banco de Células do Rio de Janeiro—BCRJ* (Rio de Janeiro, Brazil). The MDA-MB-231 and MCF-7 cells were cultured in RPMI-1640 and DMEM-F12, respectively,

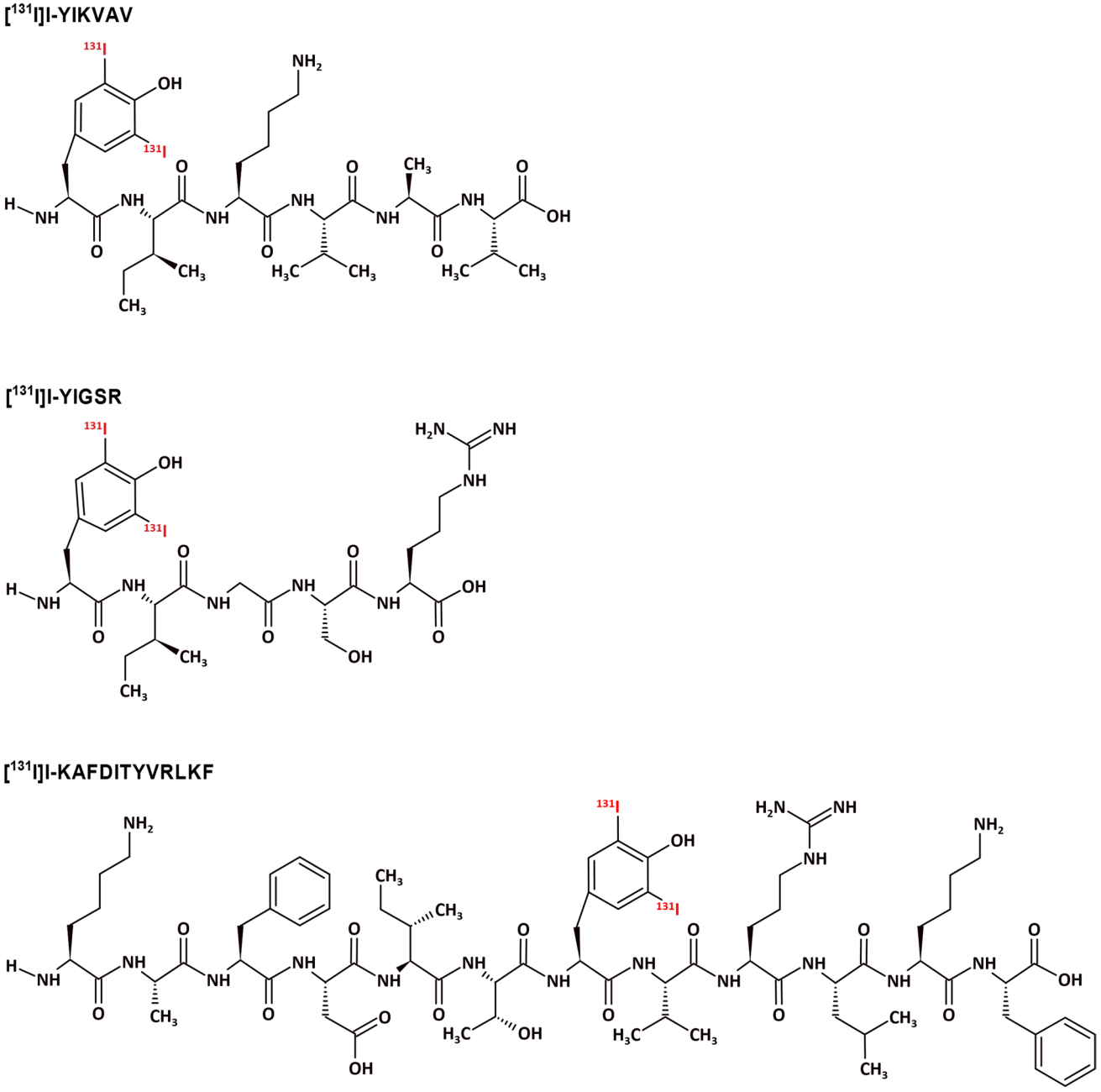

Fig. 1 ^{131}I-labeled YIKVAV, YIGSR, and KAFDITYVRLKF peptides

supplemented with 10% (v/v) fetal bovine serum and 1% (v/v) antibiotics (penicillin and streptomycin). The cells were incubated in a 5% CO_2 atmosphere, at 37 °C, and grown to a 90% confluence. Then, cells were trypsinized, centrifuged (1,500 rpm) for 5 min, and resuspended in their respective supplemented medium for the in vitro assays. For the development of the breast cancer animal model, MDA-MB-231 cells were resuspended in 1:1 matrigel:RPMI-1640 mixture.

Binding and internalization studies of the radiopeptides to MDA-MB-231 and MCF-7 tumor cells

In vials containing 2×10^6 MDA-MB-231 or MCF-7 cells resuspended in supplemented medium (450 µL), 50 µL of the [^{131}I]I-peptides (1.2 MBq) were added and incubated at 37 °C under gentle agitation (500 rpm) for 1, 4 and 24 h ($n = 5$ for each time interval). Subsequently, the vials were

centrifuged (5000 rpm) for 5 min and the supernatant was collected. The radioactivity of the cell pellet and supernatant was measured in an automatic gamma counter. The binding percentage was calculated as Eq. (3):

$$Binding\,[\%] = \frac{cpm\,(pellet)}{cpm\,(pellet + supernatant)} \times 100 \quad (3)$$

After that, the pellets were resuspended in 0.5 mL of acid buffer (0.2 mM acetic acid in 0.5 M NaCl solution; pH 2.8) and kept at room temperature for 5 min to remove radiopeptides bound to the cell membrane surface. Then, the vials were centrifuged (5000 rpm) for 5 min and the supernatant was collected. The radioactivity of the cell pellet and supernatant was measured in an automatic gamma counter. The internalization percentage was calculated as Eq. (4):

$$Internalization\,[\%] = \frac{cpm\,(pellet)}{cpm\,(pellet + supernatant)} \times 100 \quad (4)$$

MDA-MB-231 breast tumor animal model

Female Balb/c nude mice (≅20 g; ≅8 w) were supplied and maintained in the vivarium of the *Centro de Experimentação e Treinamento em Cirurgia* of the *Hospital Israelita Albert Einstein* (Sao Paulo, Brazil), accredited by the Association for Assessment and Accreditation of Laboratory Animal Care (AAALAC) International. All procedures involving mice were approved by the Ethics Committee on Animal Use of the *Hospital Israelita Albert Einstein* (protocol #3740/19).

Mice were subcutaneously inoculated into the right lower flank with 200 µL of a solution containing 1×10^7 MDA-MD-231 cells in a 1:1 matrigel:RPMI-1640 medium mixture. Tumors were allowed to grow in vivo for 30 days after inoculation or until reaching a diameter of 10 mm.

Ex vivo *biodistribution profile and autoradiography*

The ex vivo biodistribution profiles of [^{131}I]I-YIKVAV and [^{131}I]I-YIGSR were determined after intravenous injection into MDA-MB-231 breast tumor-bearing ($n = 4$) and naive ($n = 3$) female Balb/c nude mice. Animals were anesthetized using ketamine–xylazine combination (100:10 mg/Kg) and euthanized at 15 and 120 min post-injection. Organs and tissues of interest were dissected, dried on filter paper, weighed, and measured using an automatic gamma counter. A standard dose with the same amount of radioactivity as injected into the mice was counted. The results were expressed as the percentage of injected dose per gram of tissue (%ID/g). After samples counting, the tumor and contralateral muscle were used for autoradiography as previously described (de Paula Faria et al. 2023). Briefly, tissues were frozen and sliced at 30 µm in a cryostat, then were exposed to a phosphor-imaging plate (BASMS-2325; Fujifilm, Japan) for 24 hats 21–25 °C. The plate was scanned using a Typhoon FLA 9500 plate reader (GE Healthcare, USA) with a pixel resolution of 100 µm for qualitative analysis.

Statistical analysis

Quantitative data were expressed as either "mean ± standard deviation (SD)" (in vitro data) or "mean ± standard error of the mean (SEM)" (in vivo data). Pairs of groups were compared using the Student t-test. The means of three or more groups were compared by one-way Analysis of Variance (ANOVA), followed by Tukey's post hoc test. The statistical significance threshold for mean differences was set at 0.05.

Results

Peptides synthesis

The synthesized YIKVAV (α1 chain), YIGSR (β1 chain), and KAFDITYVRLKF (γ1 chain) were obtained in approximately 70% yield. The theoretical molecular weights of 693.0 g/mol (YIKVAV), 596.0 g/mol (YIGSR), and 1501.0 g/mol (KAFDITYVRLKF) were confirmed by mass spectrometry.

Radiolabeling of peptides and radiochemical stability

The three peptides were ^{131}I-labeled with radiochemical yields of 98 ± 4%, 93 ± 6%, and 80 ± 7% for [^{131}I]I-YIKVAV (0.36 MBq/nmol), [^{131}I]I-YIGSR (0.31 MBq/nmol), and [^{131}I]I-KAFDITYVRLKF (0.76 MBq/nmol), respectively ($n = 10$), determined by TLC-SG chromatography (Fig. 2). In both chromatographic systems employed in this work, free [^{131}I]NaI migrates with the mobile phase to the top of the strip ($R_f = 0.9–1.0$) and the radiolabeled peptide fragments remain at the origin of the strip ($R_f = 0.1–0.2$), allowing an efficient separation between [^{131}I]I^- and radiolabeled species. The RP-HPLC analysis (Fig. 3A) showed R_t of 15.60, 7.44, and 12.67 min for unlabeled YIKVAV, YIGSR, and KAFDITYVRLKF, respectively, while the R_t of the correspondent labeled compounds were 17.94 (Fig. 3B), 8.37 (Fig. 3C), and 15.32 min (Fig. 3D), respectively. Free [^{131}I]NaI showed R_t of 2.80 min.

The radiochemical stability of [^{131}I]I-YIKVAV, [^{131}I]I-YIGSR, and [^{131}I]I-KAFDITYVRLKF are summarized in Fig. 4. The [^{131}I]I-YIKVAV (Fig. 4A) and [^{131}I]I-YIGSR (Fig. 4B) presented suitable radiochemical stability in saline

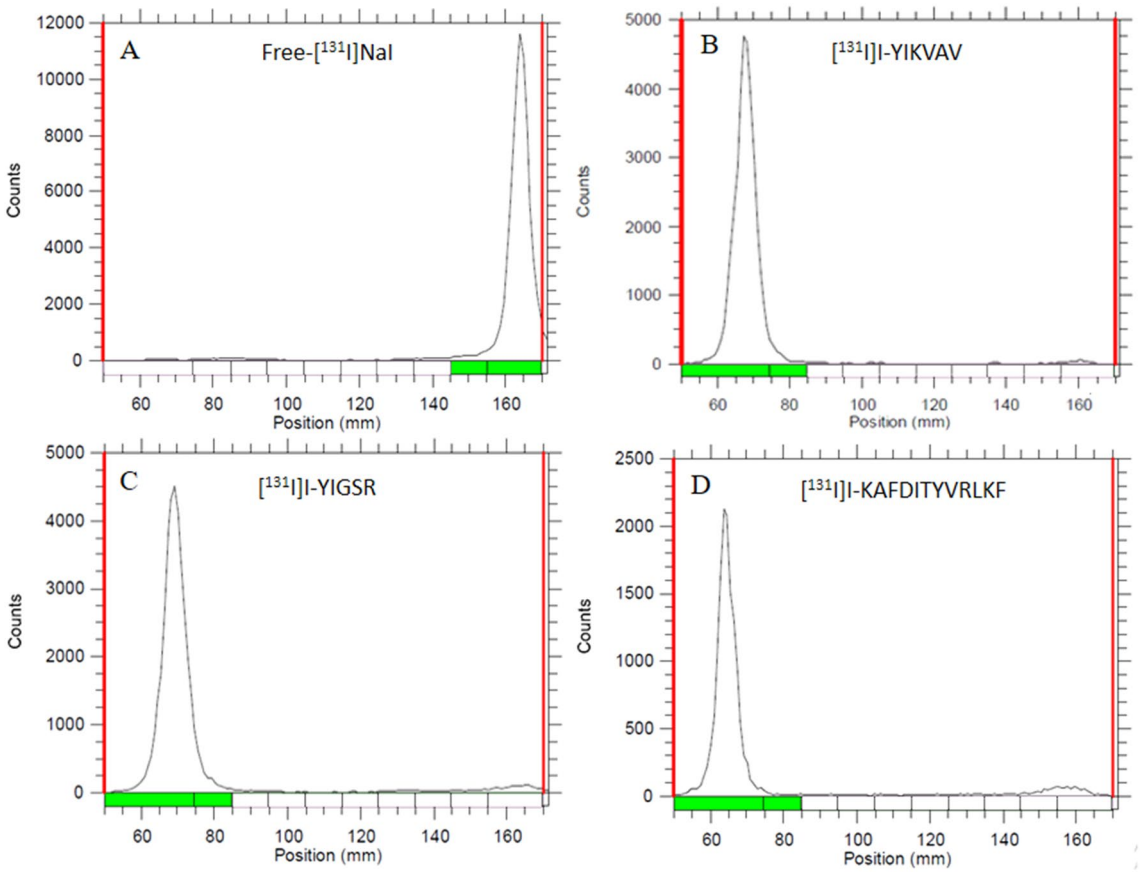

Fig. 2 Ascending radiochromatograms obtained in TLC strips using either 95:5 ACN/H_2O solution for free [^{131}I]NaI, [^{131}I]I-YIKVAV, and [^{131}I]I-YIGSR, or 0.9% NaCl solution for [^{131}I]I-KAFDITYVRLKF as eluents

and, only at 48 h post-radiolabeling, small reductions of ≅ 10 and 5%, respectively, were observed in the radiochemical purity. On the other hand, the radiochemical purity of [^{131}I]I-KAFDITYVRLKF (Fig. 4C) decreased by approximately 50% after 24 h, when maintained at room temperature or under refrigeration. The radiochemical stability was also evaluated in serum, and the results were similar to those in saline, i.e., [^{131}I]I-YIKVAV (Fig. 4A) and [^{131}I]I-YIGSR (Fig. 4B) were stable within 24 h, but [^{131}I]I-KAFDITYVRLKF (Fig. 4C) was unstable.

Lipophilicity and serum protein binding (SPB)

The lipophilicity, expressed as Log P, and the SPB percentage data are summarized in Table 1.

Biological evaluation

The affinity studies of [^{131}I]I-YIKVAV and [^{131}I]I-YIGSR were conducted in MDA-MB-231 and MCF-7 breast tumor cells (Fig. 5). The radiopeptides showed different values for the binding (Fig. 5A) and internalization (Fig. 5B) percentages to MDA-MB-231 cells. The binding percentages of [^{131}I]I-YIKVAV were between 5.67 ± 0.68 and 7.34 ± 1.17% over the evaluated time interval. The [^{131}I]I-YIGSR showed a binding percentage of 8.42 ± 0.50% at 1 h, which decreased to 5.72 ± 0.31% at 24 h. The internalization percentages of [^{131}I]I-YIKVAV and [^{131}I]I-YIGSR were 73.37 ± 3.73 and 49.70 ± 4.40%, respectively, at 1 h of incubation. Within 24 h, the internalization percentages of both [^{131}I]I-YIKVAV and [^{131}I]I-YIGSR were ≅ 52%. The radiopeptides also showed different results for the binding (Fig. 5C) and internalization (Fig. 5D) percentages to MCF-7 cells. The binding percentages of [^{131}I]I-YIKVAV to MCF-7 cell line were approximately 15% throughout the incubation period, with a higher binding percentage of 18.10 ± 1.63% at 4 h. The [^{131}I]I-YIGSR showed binding percentages from 6.67 ± 0.25% at 1 h to 10.02 ± 0.61% at 24 h. The internalization percentages of the [^{131}I]I-YIKVAV were approximately 80% within the first hours of incubation and decreased to 59.71 ± 5.57% at 24 h. However, the [^{131}I]I-YIGSR presented an internalization of approximately 40% within time.

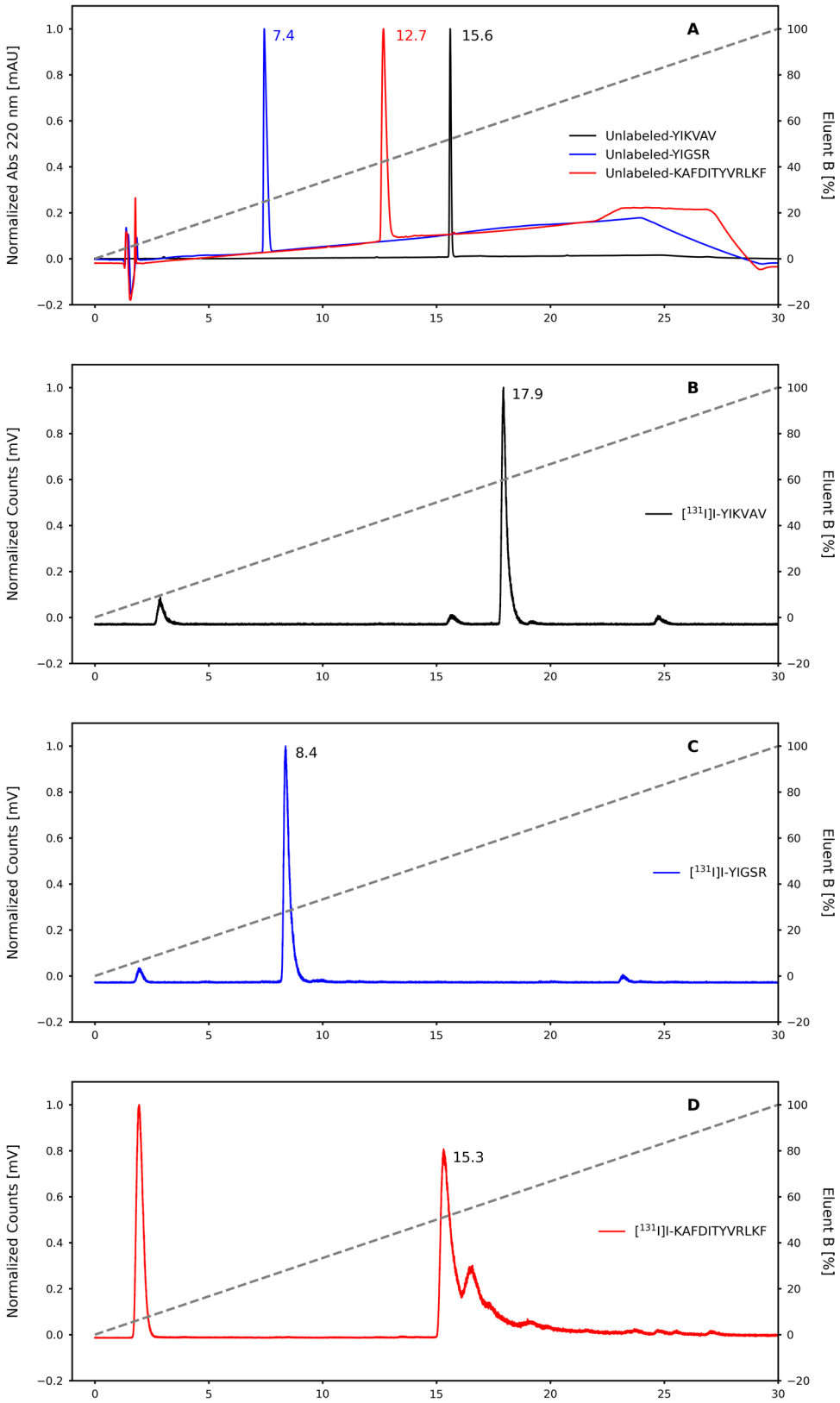

Fig. 3 RP-HPLC profiles: **A** unlabeled YIKVAV (black line), YIGSR (blue line), and KAFDITYVRLKF (red line), **B** [^{131}I]I-YIKVAV (black line), **C** [^{131}I]I-YIGSR (blue line), and **D** [^{131}I]I-KAFDITYVRLKF (red line)

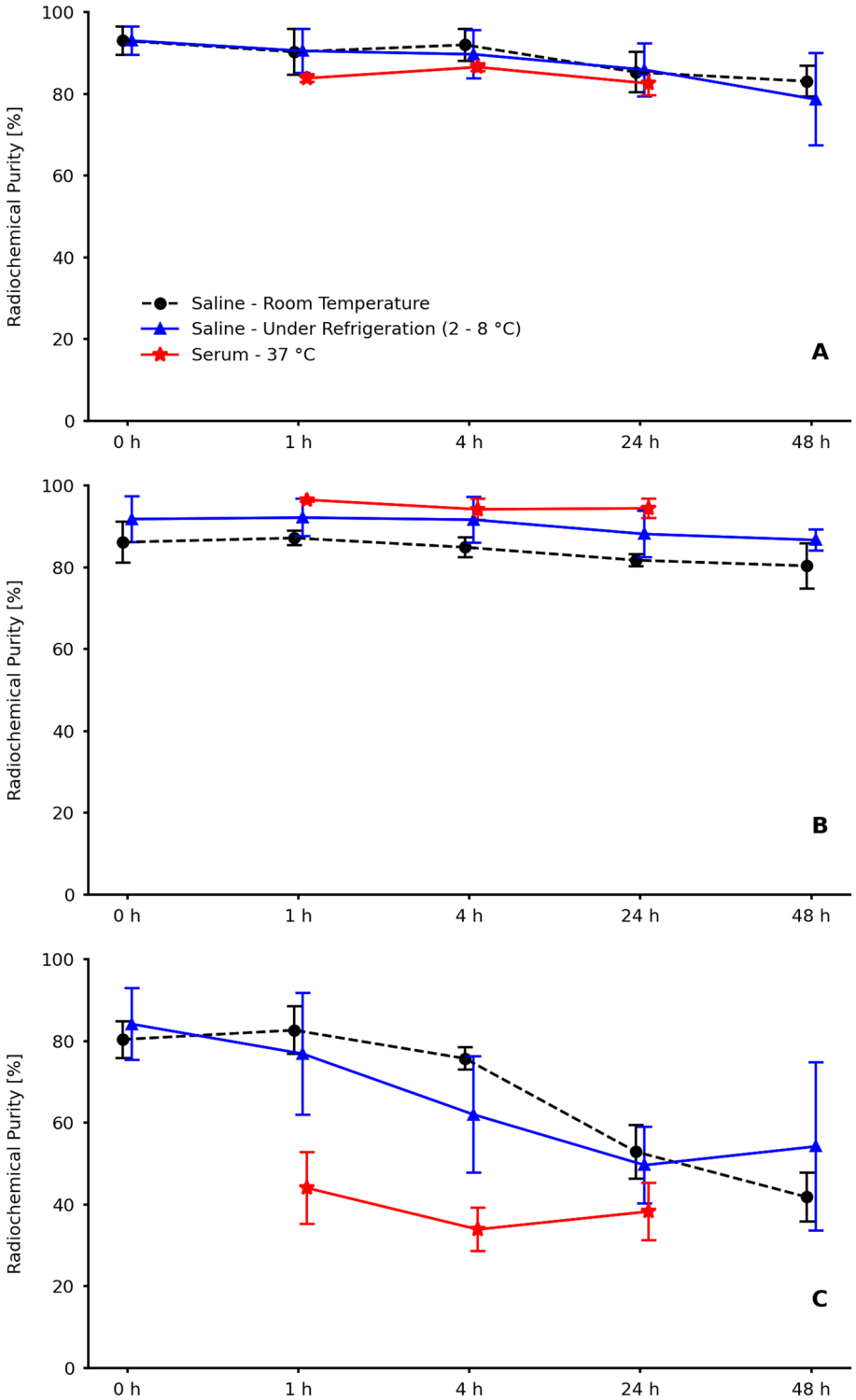

Fig. 4 Radiochemical stability in saline and serum of **A**, **B** [^{131}I]I-YIKVAV, **C**, **D** [^{131}I]I-YIGSR, and **E**, **F** [^{131}I]I-KAFDITYVRLKF. Data are expressed as 'mean ± SD' ($n = 3$ [saline]; $n = 5$ [serum]). Different letters represent statistically significant differences within time ($p < 0.05$)

The [^{131}I]I-YIKVAV and [^{131}I]I-YIGSR ex vivo biodistribution profiles are summarized in Fig. 6. Both peptides exhibited rapid blood clearance and low accumulation in non-target organs. However, there was a notable accumulation of radioactivity in the stomach and thyroid. Data obtained from xenografted mice demonstrated that [^{131}I]I-YIKVAV and [^{131}I]I-YIGSR displayed high tumor accumulation. The tumor-to-contralateral muscle ratios (Fig. 6—inserts) were 1.5 at 15 min for both peptides, which increased to 4.6 and 2.8 at 120 min for [^{131}I]I-YIKVAV and [^{131}I]I-YIGSR, respectively. These findings were further supported by autoradiography (Fig. 7), where visual analysis of

Table 1 Lipophilicity (Log P) and serum protein binding (SPB) of the three ^{131}I-labeled peptide fragments

Parameters	[^{131}I]I-YIKVAV	[^{131}I]I-YIGSR	[^{131}I]I-KAFDITYVRLKF
Log P	− 1.61 ± 0.07	− 2.12 ± 0.08	− 1.10 ± 0.04
SPB [%]	48.40 ± 0.78	25.01 ± 0.70	nd

Data are expressed as 'mean ± SD' ($n = 5$)

nd not determined

the images indicates a higher accumulation of radiopeptides in the tumor tissue than the contralateral muscle. Additionally, they were found to penetrate deeply into the tumor tissue.

Discussion

Three laminin-111-derived peptide fragments were synthesized, each representing a different chain. The IKVAV fragment represented the α1 chain, modified by introducing the non-native amino acid tyrosine (Y) at the N-terminal position to allow the radiolabeling with ^{131}I. Thus, the final structure is YIKVAV. The β1 chain was represented by the YIGSR fragment, a truncated version of the peptide CDPGYIGSR, which retained its biological activity, and the γ1 chain was represented by the C16 peptide, KAFDITYVRLKF. All fragments were synthesized using the Fmoc strategy and were purified by RP-HPLC, with chemical purity higher than 95%.

Radiolabeling of the peptides with ^{131}I was accomplished by the chloramine T method (Hunter 1970; Ebenhan et al. 2018), with the radionuclide incorporated at the aromatic ring of the tyrosine aminoacid (Fig. 1). The choice of ^{131}I in this study was influenced by its availability and cost-effectiveness.

In the radiolabeling procedure, the best radiochemical yields were achieved at 1.5, 1, and 4 min for YIKVAV, YIGSR, and KAFDITYVRLKF fragments, respectively. However, the γ1 representative, KAFDITYVRLKF, displayed a longer reaction time, likely due to steric hindrance caused by the central tyrosine residue (Fig. 1). Hu and coworkers have assessed the validity of labeling YIGSR with ^{99m}Tc by employing the bifunctional chelator S-Acetyl-NH_3-MAG3. This study achieved a radiolabeling yield of 62%

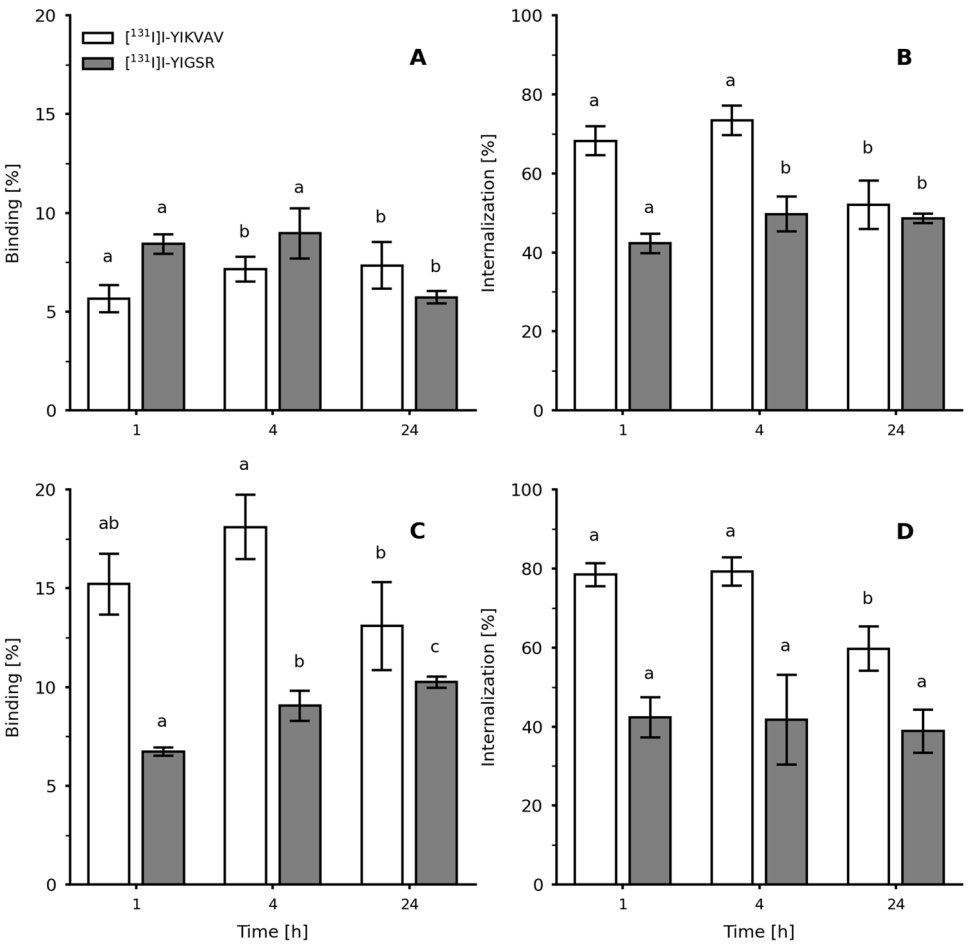

Fig. 5 Binding and internalization percentages of the [^{131}I]I-YIKVAV and [^{131}I]I-YIGSR to **A**, **B** MDA-MB-231 and **C**, **D** MCF-7 breast cancer cells. Data are expressed as 'mean ± SD' ($n = 5$). Different letters represent statistically significant differences within time for the same radiopeptide ($p < 0.05$)

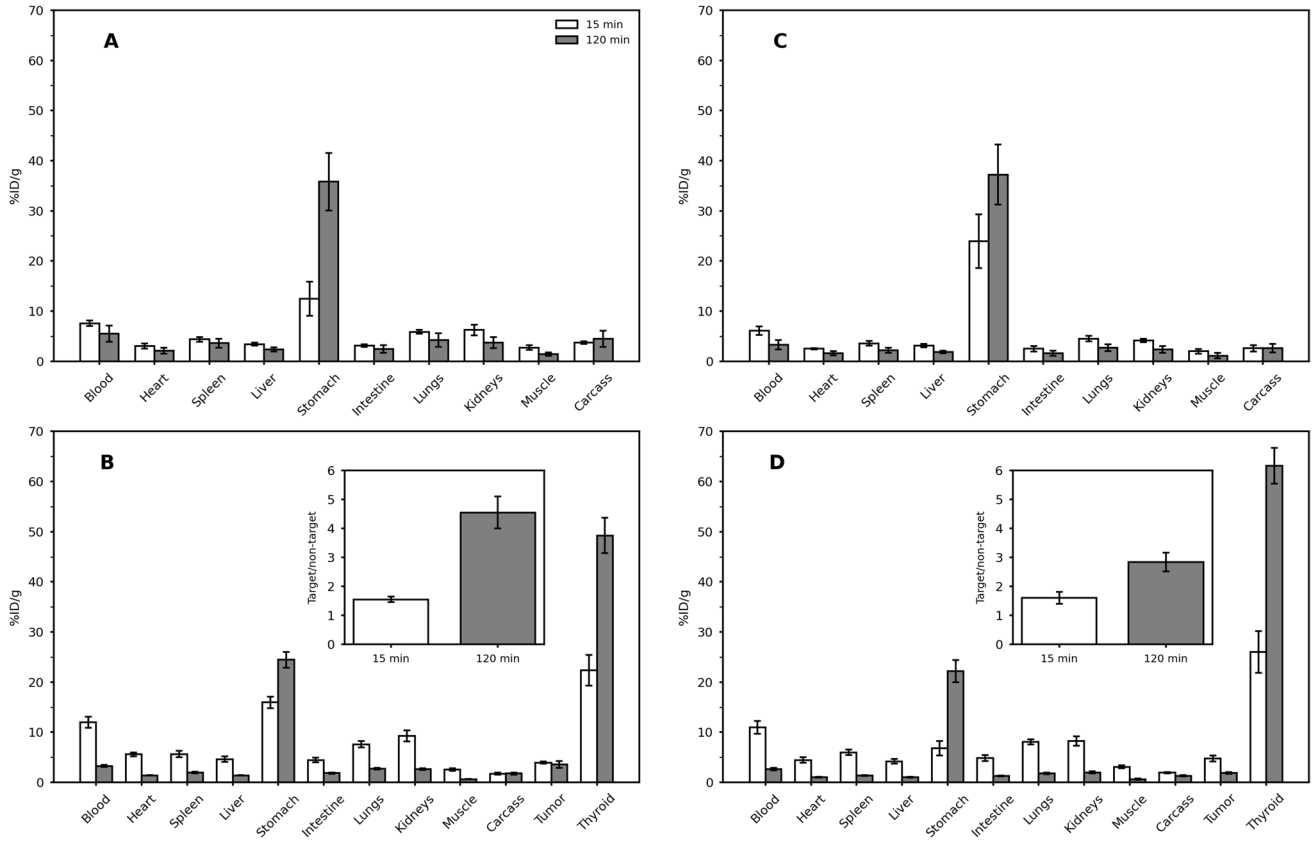

Fig. 6 Ex vivo biodistribution of **A**, **B** [^{131}I]I-YIKVAV and **C**, **D** [^{131}I]I-YIGSR in naive (control) ($n=3$) and MDA-MB-231 breast tumor-bearing nude female Balb/c mice ($n=5$–7). Inserts: Tumor-to-contralateral muscle ratios obtained from the ex vivo biodistribution data in MDA-MB-231 breast tumor-bearing nude female Balb/c mice. Data are expressed as 'mean ± SEM'

(Hu et al. 2007). Consequently, our findings demonstrated that iodine radiolabeling offers a simpler procedure and higher radiochemical efficiencies.

The use of the ascending chromatography method to evaluate radiochemical yields was motivated by its ease of use, material availability and low cost associated with the procedure, and RP-HPLC analyses validated it. Due to the delay for the samples to go through from the UV detector to the radioactivity detector, the radiopeptides exhibited slightly extended R_t when compared to the unlabeled peptide fragments. Despite this, the RP-HPLC results align with the ascending chromatographic outcomes, providing further support for the accuracy and consistency of the obtained results.

The radiochemical stability of ^{131}I-labeled peptides in saline was assessed at room temperature and under refrigeration (4–8 °C). In both conditions, the [^{131}I]I-YIKVAV and [^{131}I]I-YIGSR remained stable over time. However, the [^{131}I]I-KAFDITYVRLKF decreased radiochemical purity to around 50%, within the specified time interval, for both storage conditions. The evaluation of radiochemical stability was extended to serum at 37 °C, for 24 h. Throughout the entire duration, the [^{131}I]I-YIKVAV and [^{131}I]I-YIGSR demonstrated consistent radiochemical stability within the serum. Conversely, the [^{131}I]I-KAFDITYVRLKF exhibited radiochemical instability within the first hour of exposure to serum. The radiochemical stability is important when assessing a new peptide-based targeting molecule. Previous studies have illustrated that [^{131}I]I-peptides, across various concentrations, maintained radiochemical stability for up to 24 h following the radiolabeling procedure (Araújo et al. 2009; Brunton et al. 2010).

All the radiopeptides displayed hydrophilic characteristics, supporting preferential renal excretion, which could generate a lower background for an imaging diagnosis radiopharmaceutical. Conversely, lipophilic compounds tend to be reabsorbed and recirculated within the systemic circulation (Jeghers et al. 1990). However, due to the lower radiochemical stability of the [^{131}I]I-KAFDITYVRLKF, further evaluations were limited to the ^{131}I-labeled YIKVAV and YIGSR. This prudent decision was guided by the necessity for stable radiolabeling, a crucial factor in the evaluation and utility of radiopeptides.

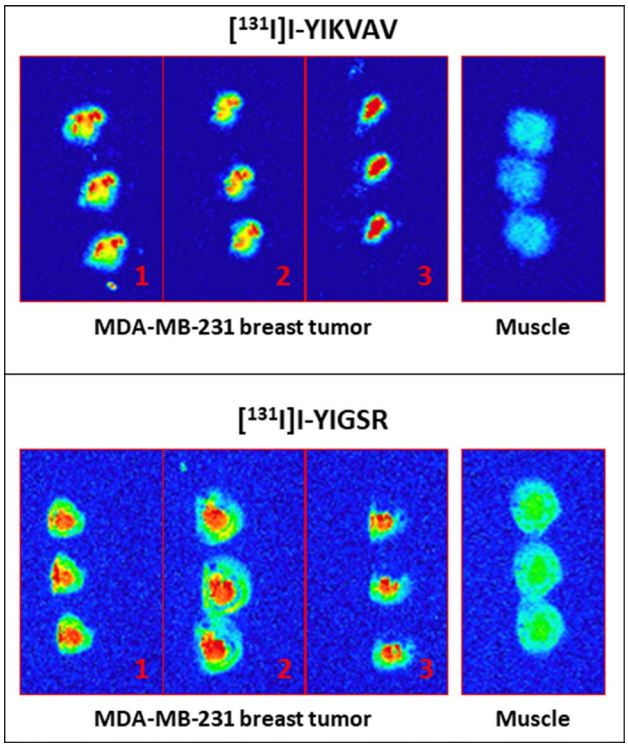

Fig. 7 Autoradiography of [^{131}I]I-YIKVAV and [^{131}I]I-YIGSR in MDA-MB-231 breast tumor-bearing mice: (1) tumor center; (2) interior of the tumor between the center and the surface; (3) tumor surface

The findings from the SPB analysis revealed that ≅ 50% of the [^{131}I]I-YIKVAV fragment and ≅ 75% of the [^{131}I]I-YIGSR are available to reach the intended target. This indicates a considerable potential for clinical application, as these fractions signify the proportion of the peptides that could potentially engage in the desired interactions or therapeutic effects (de Barros et al. 2013).

The observed variations in the binding and internalization patterns of the radiopeptides within MDA-MB-231 and MCF-7 tumor cells likely stem from the unique characteristics of each evaluated peptide. The IKVAV peptide, recognized for its role in promoting cell adhesion and migration (Bresalier et al. 1995; He et al. 2015), is likely responsible for its higher binding and internalized fractions. Due to the importance of this fragment, a recent assessment was conducted on a lyophilized matrix composed of hyaluronic acid (HA) and the IKVAV peptide within a 3D in vitro model of breast cancer. The results demonstrated that the HA-IKVAV displayed elevated sensitivity compared to its 2D counterparts, particularly regarding cellular membrane permeabilization and viability, thereby reinforcing the significance of this fragment (Sieni et al. 2020). These attributes align with its tendency to facilitate interactions that promote these cellular behaviors.

On the contrary, the YIGSR peptide is associated with angiogenesis inhibition (Ponce et al. 2003). This aligns with our findings, as this peptide demonstrated the lowest percentage of both bound and subsequently internalized fractions within a 24 h incubation period. The effectiveness of this fragment in inhibiting the growth of melanoma and lung tumor cells has been under evaluation, including metastasis formation. These studies suggested that the YIGSR peptide have a potential to be used as targeting molecule for systemic delivery for the treatment of metastatic cancer (Iwamoto et al. 1988; Sarfati et al. 2011). Moreover, this pentapeptide-rhodamine B derivative (YIGSR-RhB) exhibited high absorption by B16F10 melanoma cells and 4T1 breast cancer cells, resulting in a robust fluorescent signal within these in vitro tumor cells and in vivo mice tumors. As a result, YIGSR-RhB exhibits promising potential as a tumor-targeting probe for fluorescent imaging, displaying the ability to directly adhere to the cell membrane and selectively target tumor cells (Liu et al. 2020). In the context of our results, it is evident that the proposed peptides exhibit favorable interactions in both types of breast cancer cell lines, thereby holding promise as potential breast cancer-targeting agents.

The in vivo assay conducted in naïve and breast tumor-bearing mice demonstrated that both [^{131}I]I-YIKVAV and [^{131}I]I-YIGSR exhibited rapid blood clearance and displayed low accumulation in various non-target organs. This desirable profile indicates a minimized radioactivity background. Nevertheless, notable radioactivity accumulation was observed in the stomach and thyroid, which can be attributed to the partial in vivo release of ^{131}I from the peptides, generating free ^{131}I as a radiochemical impurity that accumulates in those organs (Lisco et al. 2023). Conversely, the peptide fraction that retained radiolabeling exhibited substantial accumulation at the tumor site. This accumulation displayed a high targeted-to-non-targeted ratio that increased from 15 to 120 min, implying a remarkable specificity for tumor tissue. Previous studies reported targeted-to-non-targeted ratios for ^{99m}Tc-labeled peptides in the same order of magnitude in a murine MCF-7 breast cancer model, however maximum tumor-to-muscle ratio was seen at 15 min post-injection. (Ahmadpour et al. 2018a, b). This specificity was further supported by autoradiography visual analysis, which illustrated higher peptide accumulation in the tumor tissue compared to the contralateral muscle at 120 min after peptide administration. Moreover, samples were obtained from various levels, ranging from the tumor surface to the center to assess the depth of penetration within the tumor tissue. These findings suggest that both YIKVAV and YIGSR peptides effectively reach and penetrate deep into the tumor tissue.

Given their promising attributes, both [^{131}I]I-YIKVAV and [^{131}I]I-YIGSR peptides are candidates for radiolabeling

with more appropriate radioisotopes. This step could enhance their performance and facilitate their evaluation as potential radiopharmaceuticals. This avenue of exploration holds significant promise for advancing their clinical utility within the realm of breast cancer imaging diagnostic and treatment, which could be achieved by further chemical modifications to enable radiolabeling with other radionuclides.

Conclusion

The YIKVAV, YIGSR and KAFDITYVRLKF peptide fragments were synthesized and radiolabeled with ^{131}I. However, due to its limited radiochemical stability, the [^{131}I]I-KAFDITYVRLKF fragment did not undergo further assessment. Conversely, the [^{131}I]I-YIKVAV and [^{131}I]I-YIGSR fragments displayed favorable radiochemical characteristics. The comprehensive in vitro and in vivo data indicated their potential as effective targeting agents for breast cancer.

Acknowledgements The authors would like to thank the *Coordenação de Aperfeiçoamento de Pessoal de Nível Superior (CAPES)* for the fellowship. Authors also thank the *Fundo de Amparo à Pesquisa (FAP)* of Santa Casa de Sao Paulo School of Medical Sciences and the grant #2021/08717-8, (CancerThera) - Sao Paulo Research Foundation (FAPESP).

Author contributions FFM: conducted all experiments. DVS: handled cell culture and preparation, as well as in vitro assays. ACRD: conducted the radiolabeling assay and quality control, including RP-HPLC analysis. ACCM: carried out the radiolabeling assay and quality control, as well as in vivo experiments. JM: prepared figures and conducted data analysis. DdPF and FLNM: both performed radioautography assays. MFdB: conducted the radiolabeling assay and quality control, and analyzed data. LLF: conducted experiments, data analysis, and provided supervision. LM: developed the project, conducted experiments, performed data analysis, and provided supervision. All authors reviewed and approved the manuscript.

Data availability The authors confirm that the data supporting the findings of this study are available within the article. Raw data that support the findings of this study are available from the corresponding authors, upon reasonable request.

Declarations

Conflict of interest The authors declare no conflict of interest.

References

Ahmadpour S, Noaparast Z, Abedi SM, Hosseinimehr SJ (2018a) ^{99m}Tc-HYNIC-(tricine/EDDA)-FROP peptide for MCF-7 breast tumor targeting and imaging. J Biomed Sci. https://doi.org/10.1186/s12929-018-0420-x

Ahmadpour S, Noaparast Z, Abedi SM, Hosseinimehr SJ (2018b) ^{99m}Tc-(tricine)-HYNIC-Lys-FROP peptide for breast tumor targeting. Anticancer Agents Med Chem. https://doi.org/10.2174/1871520618666180307142027

Araújo EB, Caldeira-Filho JS, Nagamati EM, Muramoto E, Colturato MT, Couto RM et al (2009) A comparative study of ^{131}I and ^{177}Lu labeled somatostatin analogues for therapy of neuroendocrine tumours. Appl Radiat Isot. https://doi.org/10.1016/j.apradiso.2008.09.009

Batiston AP, Tamaki EM, de Souza LA, dos Santos MLM (2011) Knowledge of and practices regarding risk factors for breast cancer in women aged between 40 and 69 years. Rev Bras Saúde Mater Infant. https://doi.org/10.1590/S1519-38292011000200007

Bosman FT, Stamenkovic I (2003) Functional structure and composition of the extracelular matrix. J Pathol. https://doi.org/10.1002/path.1437

Bresalier RS, Schwartz B, Kim YS, Duh QY, Kleinman HK, Sullam PM (1995) The laminin α1 chain Ile-Lys-Val-Ala-Val (IKVAV)-containing peptide promotes liver colonization by human colon cancer cells. Cancer Res 55:2476–2480

Brunton LL, Parker KL, Blumenthal DK, Buxton IL (2010) In: Manual de Farmacologia e Terapêutica de Goodman & Gilman, 12ª. Artmed, Rio de Janeiro, pp 04–14

De Barros ALB, Motta LG, de Aguiar CF et al (2013) 99mTc-labeled bombesin analog for breast cancer identification. J Radioanal Nucl Chem. https://doi.org/10.1007/s10967-012-2331-8

Durante AC, Sobral DV, Miranda ACC, de Almeida EV, Fuscaldi LL, de Barboza MF, Malavolta L (2019) Comparative study of two oxidizing agents, chloramine T and Iodo-Gen®, for the radiolabeling of β-CIT with Iodine-131: relevance for Parkinson's disease. Pharmaceuticals. https://doi.org/10.3390/ph12010025

Ebenhan T, Sathekge MM, Lengana T, Koole M, Gheysens O, Govender T, Zeevaart JR (2018) ^{68}Ga-NOTA-funcionalizada ubiquicidina: citotoxicidade, biodistribuição, dosimetria de radiação e primeira imagem PET/CT humana de infecções. J Nucl Med 12:25–29. https://doi.org/10.2967/jnumed.117.200048

Faria DP, Campeiro JD, Junqueira MS, Real CC, Marques FLN, Hayashi MAF, Sapienza MT (2023) [^{18}F]FDG and [^{11}C]PK11195 PET imaging in the evaluation of brown adipose tissue – effects of cold and pharmacological stimuli and their association with crotamine intake in a male mouse model. Nucl Med Biol. https://doi.org/10.1016/j.nucmedbio.2023.108362

Ferlay J, Colombet M, Soerjomataram I, Parkin DM, Piñeros M, Znaor A, Bray F (2021) Cancer statistics for the year 2020: An overview. Int J Cancer. https://doi.org/10.1002/ijc.33588

Fields GB, Noble RL (1990) Solid-phase peptide-synthesis utizing 9-fluorenylmethoxycarbonyl amino-acids. Int J Pept Prot Res 35:161–214

Hamill KJ, Kligys K, Hopkinson SB, Hopkinson SB, Jones JC (2009) Laminin deposition in the extracellular matrix: a complex picture emerges. J Cell Sci. https://doi.org/10.1242/jcs.041095

Hanahan D, Weinberg RA (2011) Hallmarks of cancer: the next generation. Cell. https://doi.org/10.1016/j.cell.2011.02.013

He X, Hao Y, Long W, Song N, Fan S, Meng A (2015) Exploration of peptide T7 and its derivative as integrin $\alpha_V\beta_3$-targeted imaging agents. Onco Targets Ther. https://doi.org/10.2147/OTT.S82095

Hu J, Qin G, Zhang Y, An R, Lan X (2007) ^{99m}Tc-YIGSR as a receptor tracer in imaging the Ehrlich Ascites tumor-bearing mice

as compared with ^{99m}Tc-MIBI. J Huazhong Univ Sci Technol. https://doi.org/10.1007/s11596-007-0432-3

Hunter R (1970) Standardization of the chloramine-T method of protein iodination. Proc Soc Exp Biol Med 133:989–992

Iwamoto Y, Robey FA, Graf J, Sasaki M, Kleinman HK, Yamada Y, Martin GR (1988) YIGSR, a synthetic laminin pentapeptide, inhibits experimental metastasis formation. Science. https://doi.org/10.1126/science.2961059

Jeghers O, Piepz A, Ham HR (1990) What does protein binding of radiopharmaceuticals mean exactly? Eur J Nucl Med 17:101–102

Kaiser E, Colescot RI, Bossinge CD, Cook PI (1970) Color test for detection of free terminal amino groups in solid-phase synthesis of peptides. Anal Biochem 34:595–598

Kikkawa Y, Hozumi K, Katagiri F, Nomizu M, Kleinman HK, Koblinski JE (2013) Laminin-111-derived peptides and cancer. Cell Adh Migr. https://doi.org/10.4161/cam.22827

Lisco G, De Tullio A, Triggiani D, Zupo R, Giagulli VA, De Pergola G, Piazzolla G, Guastamacchia E, Sabbà C, Triggiani V (2023) Iodine Deficiency and iodine prophylaxis: an overview and update. Nutrients. https://doi.org/10.3390/nu15041004

Liu F, Yan JR, Chen S, Yan GP, Pan BQ, Zhang Q, Wang YF, Gu YT (2020) Polypeptide-rhodamine B probes containing laminin/fibronectin receptor-targeting sequence (YIGSR/RGD) for fluorescent imaging in cancers. Talanta. https://doi.org/10.1016/j.talanta.2020.120718

Mokotoff M, Swanson DP, Jonnalagadda SS, Epperly MW, Brown ML (1997) Evaluation of laminin peptide fragments labeled with indium-111 for the potential imaging of malignant tumors. J Pept Res. https://doi.org/10.1111/j.1399-3011.1997.tb01158.x

Montor WR, Salas AROSE, Melo FHM (2018) Receptor tyrosine kinases and downstream pathways as druggable targets for cancer treatment: the current arsenal of inhibitors. Mol Cancer. https://doi.org/10.1186/s12943-018-0792-2

Otagiri D, Yamada Y, Hozumi K, Katagiri F, Kikkawa Y, Nomizu M (2013) Cell attachment and spreading activity of mixed laminin peptide-chitosan membranes. Pept Sci. https://doi.org/10.1002/bip.22303

Ponce ML, Nomizu M, Kleinman HK (2001) An angiogenic laminin site and its antagonist bind through the $\alpha_V\beta_3$ and $\alpha_V\beta_1$ integrins. FASEB J. https://doi.org/10.1096/fj.00-0736com

Ponce ML, Hibino S, Lebioda AM, Mochizuki M, Nomizu M, Kleinman HK (2003) Identification of a potent peptide antagonist to active laminin-1 sequences and angiogenesis and tumor growth. Cancer Res 63:5060–5064

Sarfati G, Dvir T, Elkabets M, Apte RN, Cohen S (2011) Targeting of polymeric nanoparticles to lung metastases by surface-attachment of YIGSR peptide from laminin. Biomaterials. https://doi.org/10.1016/j.biomaterials.2010.09.014

Schottelius M, Wester HJ (2009) Molecular imaging targeting peptide receptors. Methods. https://doi.org/10.1016/j.ymeth.2009.03.012

Sieni E, Bazzolo B, Pieretti F, Zamuner A, Tasso A, Dettin M, Conconi MT (2020) Breast cancer cells grown on hyaluronic acid-based scaffolds as 3D in vitro model for electroporation. Bioelectrochem. https://doi.org/10.1016/j.bioelechem.2020.107626

Smuczek B, Santos ES, Siqueira AS, Pinheiro JJV, Freitas VM, Jaeger RG (2017) The laminin-derived peptide C16 regulates GPNMB expression and function in breast cancer. Exp Cell Res. https://doi.org/10.1016/j.yexcr.2017.07.005

Sobral DV, Fuscaldi LL, Durante ACR, Rangel MG, Oliveira LR, Mendonça FF, Miranda ACC, Cabeza JM, Montor WR, Cabral FR, Barboza MFF, Malavolta L (2020) Radiochemical and biological properties of peptides designed to interact with EGF receptor: relevance for glioblastoma. Nucl Med Biol. https://doi.org/10.1016/j.nucmedbio.2020.07.001

De Souza ES (2011) Microarray analysis of differentially expressed genes in breast cancer cell lines (MDA-MB-231) treated with the bioactive peptide of laminin C16. Dissertation, Institute of Biomedical Sciences, University of Sao Paulo

Sweeney TM, Kibbey MC, Zain M, Fridman R, Kleinman HK (1991) Basement membrane and the SIKVAV laminin-derived peptide promote tumor growth and metastases. Cancer Metastasis Rev. https://doi.org/10.1007/BF00050795

Tashiro K, Sephel GC, Weeks B, Sasaki M, Martin GR, Kleinman HK, Yamada Y (1989) A synthetic peptide containing the IKVAV sequence from the A chain of laminin mediates cell attachment, migration, and neurite outgrowth. J Biol Chem. https://doi.org/10.1016/S0021-9258(18)71604-9